Rare Metal Materials and Engineering
Volume 49, Issue 2, February 2020
Available online at www.rmme.ac.cn

Science Press

Cite this article as: Rare Metal Materials and Engineering, 2020, 49(2): 0422-0428.

ARTICLE

Microstructure and Thermophysical Properties of Hot-pressed Cu/FeCoCr Composites

Liu Xingjun[1,2], Zhu Jiahua[1], He Zhoufeng[1], Zhang Jinbin[1], Yang Shuiyuan[1], Han Jiajia[1], Lu Yong[1], Wang Cuiping[1]

[1] Fujian Provincial Key Laboratory of Materials Genome, Xiamen University, Xiamen 361005, China; [2] Harbin Institute of Technology, Shenzhen 518055, China

Abstract: Series of micro-scale powders with composite microstructure based on CuFeCoCr system were successfully designed and fabricated using CALPHAD approach (calculated from phase diagrams) and gas atomization method. The bulk CuFeCoCr composites were produced by hot pressing technique at 950 °C under a pressure of 45 MPa. The effect of Cu content on the microstructure, coefficient of thermal expansion (CTE), thermal conductivity (TC) and micro-hardness (HV) were systematically studied. The results show that the CuFeCoCr composites present a microstructure of two separate fcc phases (Cu-rich and FeCrCo-rich phase). After annealing at 500 °C for 8 h, the CTE of the composites ranges from 5.83×10^{-6}~10.61×10^{-6} K^{-1} and TC varies from 42.17 $W\cdot m^{-1}\cdot K^{-1}$ to 107.53 $W\cdot m^{-1}\cdot K^{-1}$. Particularly, the $Cu_{55}(Fe_{0.37}Cr_{0.09}Co_{0.54})_{45}$ composite exhibits excellent comprehensive properties, i.e. CTE of 9.08×10^{-6} K^{-1} and TC of 91.09 $W\cdot m^{-1}\cdot K^{-1}$, which match well with the properties of semiconductors for electronic packaging.

Key words: CALPHAD approach; composites; liquid phase separation; thermal expansion coefficients; thermal conductivity

In past decades, with the development of the electronic products, the continuing increase in electronic packaging density leads to the demand for materials with special properties[1-4]. For example, to minimize thermal stresses which can cause component or solder failure, and packaging materials must have coefficient of thermal expansion (CTE) matching the substrates and semiconductors (such as Al_2O_3, AlN, Si and GaAs)[5,6]. Further, in order to reduce the heat generated during the component working, a high thermal conductivity (TC) of the packaging materials is required. In addition, low cost and good mechanical performance should also be considered.

As traditional metal packaging materials (such as Al, Cu, steel, Invar and Kovar alloys[6-9]) used in electronic packaging cannot meet all these requirements. Therefore, new composite materials will be good candidates for electronic packaging materials such as combining different materials with high TC and low CTE by unique preparation method.

During past decades, numerous composites used for electronic packaging are presented[10-14]. One typical composite material (SiC_p/Al) for electronic packaging has been successfully prepared and widely used[10,11]. However, poor processing and welding properties affect the application of SiC_p/Al. After that, a novel low CTE and high TC composite, i.e. Cu/Invar/Cu (CIC), with multilayer structures has been obtained by cold-rolling Cu and Invar alloy sheets together[15,16]. Although CIC composite has partially replaced some thermal management materials (Kovar alloy, FeNi42 and Mo(W)-Cu alloys), there are still some disadvantages, i.e. obvious anisotropy in different directions and the weak interfacial strength. Therefore, a Cu/Invar composite with various advantages was prepared by powder metallurgy (PM) process[17,18]. Wu et al[18] also prepared Cu/Invar composites with different Cu contents varying from 30% to 50% by PM

Received date: February 12, 2019
Foundation item: National Natural Science Foundation of China (51471138)
Corresponding author: Wang Cuiping, Ph. D., Professor, Fujian Provincial Key Laboratory of Materials Genome, College of Materials, Xiamen University, Xiamen 361005, P. R. China, Tel: 0086-592-2180606, E-mail: wangcp@xmu.edu.cn

method. In the previous works, there are two key issues in the preparation of the Cu/Invar composites. First, low density and high sintering temperature (~1000 °C), due to the low sintering activity of Invar alloy, so high sintering temperature is required to improve the relative density of the bulk composites. Second, there are three kinds of sintering interfaces (Cu/Cu, Cu/Invar and Invar/Invar) and obvious agglomeration phenomenon of powders, which result in the deterioration of the physical properties of the bulk composites. Hence, exploration on other preparation methods is definitely needed.

The purpose of present study is to prepare Cu-FeCoCr composite powder, which contains a unique microstructure induced by liquid phase separation phenomenon, using gas atomization method. And then, bulk composite materials were synthesized through hot pressing technique. Lastly, the microstructure, CTE, TC and microhardness were systematically investigated.

1 Experiment

1.1 Alloy design

According to the super-Invar alloy of the reported Fe37Co54Cr9 (wt%) alloy, a vertical section diagram of the CuFeCoCr system for the composition cut between pure Cu and Fe37Co54Cr9 was calculated, as shown in Fig.1. The thermodynamics database for present calculation is from the Cu-based alloys constructed by our group[19,20]. From Fig.1, it can be seen that there is a stable liquid-liquid phase separation region (L1+L2) with large composition range. A large two fcc phases (fcc-Cu and fcc-(Fe, Ni, Co)) equilibrium region constitute the main feature in the system. It is worth noting that the solid solubility of two fcc phases is reduced with decreasing the temperature, which may be useful for further annealing process. Using the two fcc phases equilibrium region, four alloys with a composition of $(Fe_{0.37}Co_{0.54}Cr_{0.09})_{100-x}Cu_x$ (x=30, 45, 55, 65, wt%) were selected.

1.2 Materials

High purity elements of Fe, Co, Cr and Cu (≥99.9 wt%) with nominal composition of $Cu_x(Fe_{0.37}Co_{0.54}Cr_{0.09})_{100-x}$ (x=30, 45, 55, 65, wt%) were firstly melted in high frequency induction furnace under an argon atmosphere. The powders with 10~250 μm in diameter were prepared using conventional nitrogen gas atomization under a pressure of about 5 MPa. The bulk Cu/FeCoCr composites were prepared by powder metallurgy method. The green compact was consolidated in a graphite mold by hot press sintering at 950 °C under a pressure of 80 MPa for 2 h in vacuum (1.0×10^{-3} Pa). The fabricated composites with x=30, 45, 55, 65 were referred to as Cu30, Cu45, Cu55 and Cu65, respectively.

1.3 Analysis techniques

Microstructures of the powders and composites were investigated by electron probe micro-analyzer (EPMA) (JXA-8100R, JEOL, Japan). The composition of the prepared powders was measured by EPMA-WDS. Pure elements of Fe, Co, Cr and Cu were used as internal standards and EPMA was performed at 20 kV. The phase structure of the composite was identified by X-ray diffraction (XRD) using a PANalytical X'pert PRO with Cu Kα radiation at 40.0 kV and 40 mA. The data were collected in the 2θ range of 30°~95° with a step of 0.0167°. The bulk density of the composites was measured using a method based on Archimedes' law and compared with the theoretical density. The measurement of the CTE was performed by a Netzsch dilatometer in the temperature range from 25 °C to 200 °C at a heating rate of 5 °C·min^{-1} under argon atmosphere. By measuring the relationship between the size change of the sample (dl/L_0) and the temperature, the slope of the measured curve is defined as CET. Thermal conductivity was measured using laser flash method in LFA447 laser thermal conductivity analyzer from Netzsch, Germany. The samples were cut into disc-shaped with a diameter of 10 mm and a thickness of 2 mm. Vickers hardness of the samples was measured on a microhardness tester under a load of 2 kg and a dwell time of 15 s.

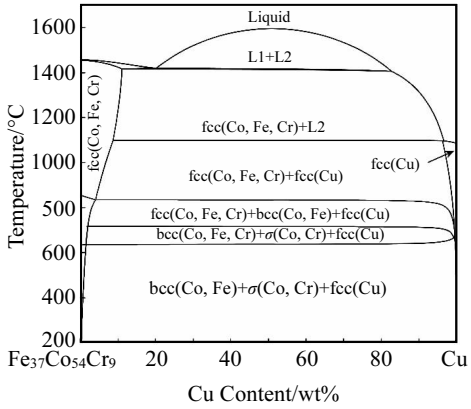

Fig.1 Calculated vertical section of the Cu-Fe-Co-Cr quaternary system for the composition cut between Fe37Co54Cr9 (wt%) and pure Cu

2 Results and Discussion

Fig.2 shows the cross-sectional microstructures of the prepared composite powders. It can be seen that all the prepared alloy powders present a composite microstructure containing two phases of white and grey phases. In addition, with the increase of Cu content, the fraction of the white phase increases gradually, implying that the microstructures of these alloy powders are closely related to the Cu content, which can be understood from the calculated vertical section phase diagram of Fe37Co54Cr9-Cu (Fig.1). In the Cu55 and Cu 65 samples shown in Fig.2c and 2d, respectively, the gray contrast phase exhibits multi-sized circular globules dispersed in the continuous white matrix. The interface between the two phases is very smooth, which demonstrates that this composite

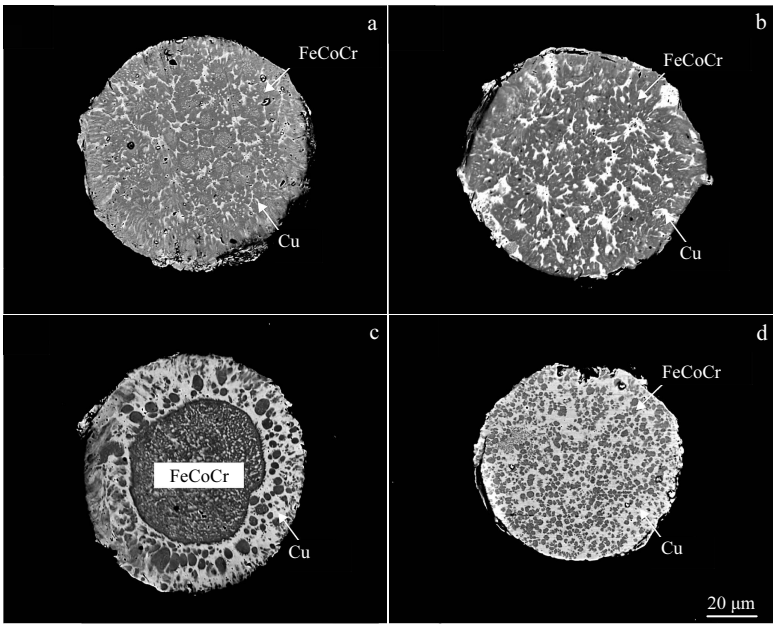

Fig.2 Cross-sectional microstructures of $Cu_x(Fe_{0.37}Co_{0.54}Cr_{0.09})_{100-x}$ (x=30, 40, 55, 65, wt%) composite powders: (a) x=30, (b) x=40, (c) x=55, and (d) x=65

microstructure is obtained through liquid phase separation phenomenon. The similar microstructure was also observed in our previous studies on liquid immiscible gas-atomized powders[21-24]. To analyze the composition of the white and grey phases, EPMA-WDS analysis was conducted. The average composition of the white and gray phases of present composite powders is listed in Table 1. From Table 1, it can be confirmed that the gray phase is rich in Fe, Co, and Cr, while the white phase mainly contains Cu. This can be explained by the mixing enthalpy of atomic pairs in Fe-Co-Cr-Cu system[25]. The positive mixing enthalpy of the Fe-Cu, Co-Cu and Cr-Cu pairs and the larger negative enthalpies of Fe-Cr, Fe-Co and Co-Cr pairs imply that the homogeneous liquid is separated into FeCoCr-rich and Cu-rich liquid phases[25]. Furthermore, it is also found that the mass ratio of Fe:Co:Cr in the FeCoCr-rich phase is approximately 37.5:53.7:8.8, close to Fe:Co:Cr mass percentage of 37:54:9 in super-Invar alloy.

The XRD patterns of the CuFeCoCr composite powders with different Cu contents are shown in Fig.3. The super strong and sharp diffraction peaks of fcc-type microstructures which are corresponding to Cu-rich and FeCoCr-rich phases can be observed in all powders. Meanwhile, the intensity of Cu-rich diffraction peaks significantly increases with increasing the Cu content, while FeCoCr diffraction peaks present an imperceptible increase. This is also consistent with the change of the volume fraction of Cu-rich and FeCoCr-rich phases with Cu content. In addition, there is no other phases can be observed in the composite powders.

Metallographic results are shown in Fig.4. Buk CuFeCoCr composites with different composition were observed by a low powered microscope. All the composites have high relative density of about 99% (Table 2) and no obvious voids are observed. In the Cu30 and Cu45 samples containing low Cu content, the FeCoCr-rich phase (gray) is spherically distributed while segregation phenomenon appears in the Cu-rich phase (white). This is caused by the inhomogeneous distribution of Cu-rich phase on the surface of composite powders. With the increase of Cu content (Cu55 and Cu65 composites), the size of FeCoCr-rich phase decreases gradually and it is uniformly embedded in the Cu-rich matrix, as shown in Fig.4c and 4d. The uniform and tiny metallurgical structure indicates that the sintering process is perfect. The composition of the Cu-rich and FeCoCr-rich phases in the composites is listed in Table 3. In this Table, it can be found that the

Table 1 Average composition of the $Cu_x(Fe_{0.37}Co_{0.54}Cr_{0.09})_{100-x}$ (x=30, 40, 55, 65, wt%) composite powders in Fig.2

Alloys	Constituted phases	Cu-rich phase/wt%				FeCoCr-rich phase/wt%			
		Cu	Co	Fe	Cr	Cu	Co	Fe	Cr
Cu30	Cu-rich+FeCoCr-rich	89.2	6.1	3.9	0.8	14.1	46.1	32.0	7.8
Cu40	Cu-rich+FeCoCr-rich	89.6	5.8	3.8	0.8	14.8	45.8	31.9	7.5
Cu55	Cu-rich+FeCoCr-rich	90.5	5.7	3.1	0.7	14.6	45.7	32.3	7.4
Cu65	Cu-riche+FeCoCr-rich	91.9	4.7	2.8	0.6	15.3	45.3	32.1	7.3

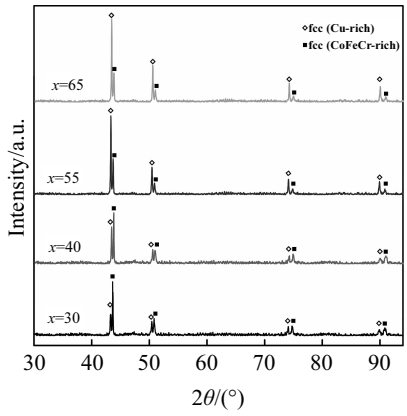

Fig.3 XRD patterns of $Cu_x(Fe_{0.37}Co_{0.54}Cr_{0.09})_{100-x}$ (x=30, 40, 55, 65, wt%) composite powders

composition of two phases is almost the same as that of the composite powder.

Fig.5 compares the size change dl/L_0 vs temperature result of the synthesized bulk Cu/FeCoCr composites. It can be seen that the dl/L_0 of all samples shows a linear relationship at 25~200 °C. The slope of the line in Fig.5 is defined as CET. In order to reduce the effect of residual stress on CTE of bulk Cu/FeCoCr composites, all samples were annealed at 500 °C for 8 h. Fig.6 shows the dl/L_0 results of bulk composites before and after annealing treatment. Interestingly, it can be found that the CTE of all composites decreases obviously after annealing treatment (as shown in Table 3). For example, the CET of alloy Cu55 is reduced from 10.35×10^{-6} K^{-1} to 9.08×10^{-6} K^{-1}; TC of alloy Cu55 is 91.09 $W\cdot m^{-1}\cdot K^{-1}$ after annealing treatment.

In general, there are two models for predicting the CTE of the composites, which are a simple rule of mixtures (ROM) and Turner's model[26]. The ROM model gives the thermal expansion coefficient α_c of a composite as follows:

$$\alpha_c = \alpha_1 V_1 + \alpha_2 V_2 \quad (1)$$

Differences in thermal expansion coefficient of the components in a composite or multiple phase alloy system can give rise to thermally induced stresses, which can influence the CTE of the composite. For this reason, the most commonly

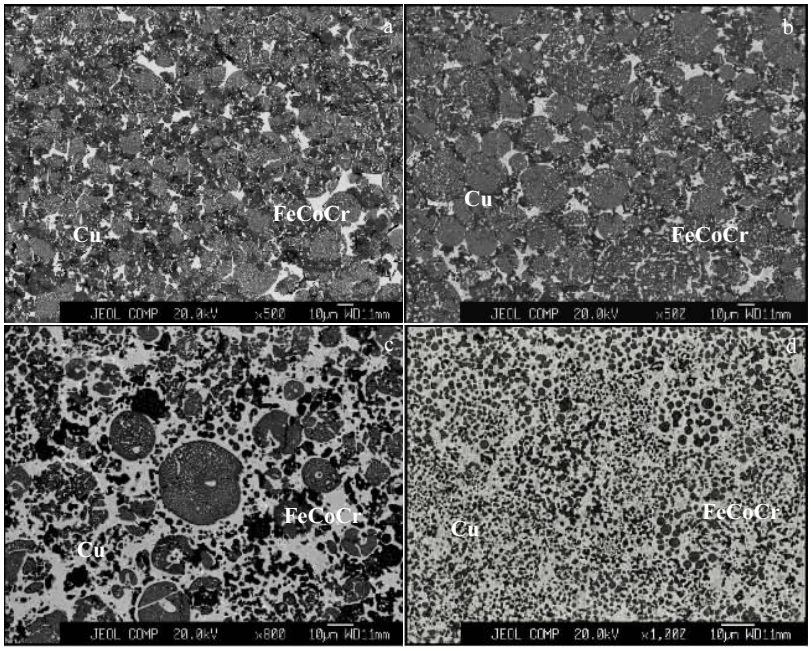

Fig.4 Metallographic microstructures of sintered $Cu_x(Fe_{0.37}Co_{0.54}Cr_{0.09})_{100-x}$ (x=30, 40, 55, 65, wt%) composite powders: (a) x=30, (b) x=40, (c) x=55, and (b) x=65

Table 2 Parameters of sintered $Cu_x(Fe_{0.37}Co_{0.54}Cr_{0.09})_{100-x}$ (x=30, 40, 55, 65, wt%) composite powders before and after annealing treatment

Alloys	Relative density/%	CTE/$\times10^{-6}$ K^{-1}		TC/$W\cdot m^{-1}\cdot K^{-1}$		HV/×10 MPa	
		Before annealing	After annealing	Before annealing	After annealing	Before annealing	After annealing
Cu30	99.07	7.21	5.83	33.66	42.17	264±15	232±15
Cu40	99.42	8.18	6.72	44.95	56.44	225±10	199±10
Cu55	99.49	10.35	9.08	68.71	91.09	184±10	170±10
Cu65	99.34	11.21	10.61	78.81	107.53	174±10	160 ±15

Table 3 Phase composition of the hot-pressing sintered $Cu_x(Fe_{0.37}Co_{0.54}Cr_{0.09})_{100-x}$ (x=30, 40, 55, 65, wt%) composite powders

Alloys	Relative density/%	Constituted phases	Cu-rich phase/wt%				FeCoCr-rich/wt%			
			Cu	Co	Fe	Cr	Cu	Co	Fe	Cr
Cu30	99.07	Cu-rich + FeCoCr-rich	93.7	3.7	2.1	0.5	11.4	46.7	33.3	8.6
Cu40	99.42	Cu-rich + FeCoCr-rich	94.2	3.5	1.9	0.4	11.8	46.5	33.5	8.2
Cu55	99.49	Cu-rich + FeCoCr-rich	94.5	3.3	1.9	0.3	12.0	46.8	33.2	8.0
Cu65	99.34	Cu-rich + FeCoCr-rich	94.6	3.3	1.8	0.3	13.2	46.4	33.0	7.4

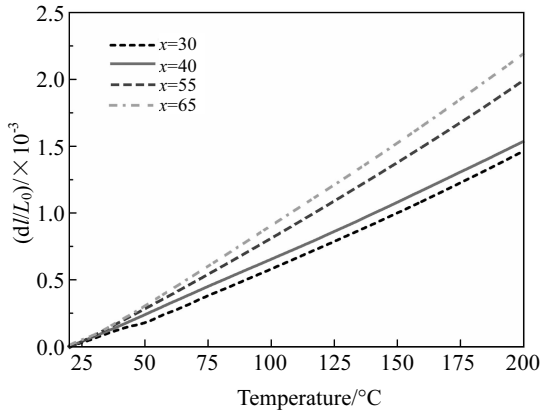

Fig.5 Thermal expansion curves of sintered $Cu_x(Fe_{0.37}Co_{0.54}Cr_{0.09})_{100-x}$ (x=30, 40, 55, 65, wt%) composite powders

used procedure for the prediction of CTE in two-phase alloys is the Turner's model[26], which gives the thermal expansion coefficient α_c of a composite as:

$$\alpha = \frac{\alpha_1 V_1 E_1 + \alpha_2 V_2 E_2}{V_1 E_1 + V_2 E_2} \quad (2)$$

where α_1 and α_2, V_1 and V_2, E_1 and E_2 are the thermal expansion coefficients (17×10^{-6} K^{-1} for Cu and 0.5×10^{-6} K^{-1} for Fe37Co54Cr9), volume fractions, and elastic modulus (110 GPa for Cu and 145 GPa for Fe37Co54Cr9) of the constituent phases, respectively. Turner's model can account for the changes of CTE caused by thermally induced stresses.

The average CTE values at the temperatures of 25~100 °C of all composites before and after annealing treatment are plotted in Fig.7, including the curves predicted by ROM and Turner's models. It can be seen that with the increase of Cu content, the CTE of all samples increases before and after

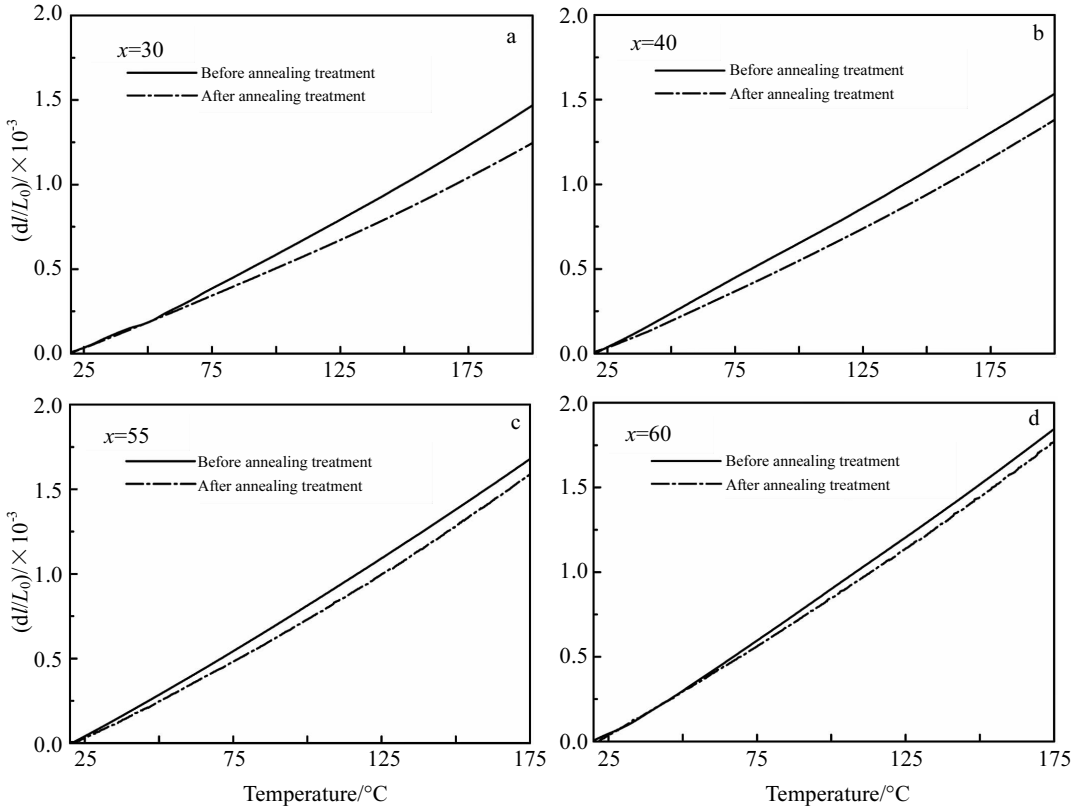

Fig.6 Thermal expansion curves of sintered $Cu_x(Fe_{0.37}Co_{0.54}Cr_{0.09})_{100-x}$ (x=30, 40, 55, 65, wt%) composite powders before and after annealing treatment

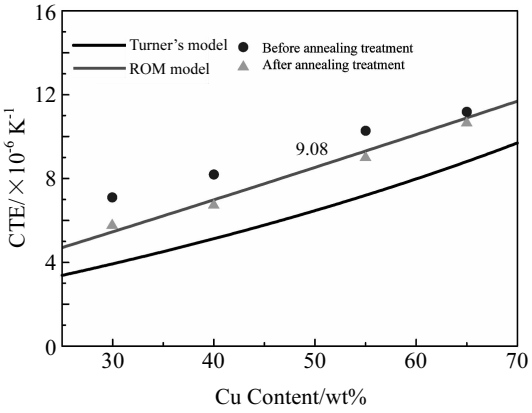

Fig.7 Comparison between experimental and theoretical CTE values of $Cu_x(Fe_{0.37}Co_{0.54}Cr_{0.09})_{100-x}$ (x=30, 40, 55, 65, wt%) composite powders sintered

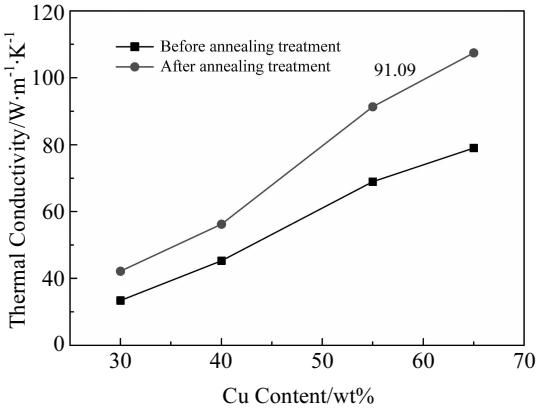

Fig.8 Thermal conductivities of $Cu_x(Fe_{0.37}Co_{0.54}Cr_{0.09})_{100-x}$($x$=30, 40, 55, 65, wt%) sintered composite powders before and after annealing treatment

annealing treatment. Compared to values predicted by Turner's model, average CTE value of the present composites matches well with the value predicted by ROM model. Most notably, average CTE value of the composites is higher than that predicted by Turner's model. This is attributed to the fact that composition of the FeCoCr-rich phase in the composites is deviated from the composition of the FeCoCr Invar alloy. It is generally known that Invar effects are very sensitive to the composition. The unique low CTE of Invar alloy is only maintained if the Fe:Co:Cr mass ratio is very close to 37:54:9. On the one hand, the Fe:Co:Cr ratio in the FeCoCr-rich phase of the composites is 37.5:53.7:8.8, which is different from the ideal value. On the other hand, it is also found that there are certain amounts of solid solution of Cu in FeCoCr-rich phase or Fe, Cr and Co in Cu-rich phase (as shows in Fig.1), which will also cause a dramatic increase in the CTE of the composites.

Fig.8 presents the changes of TC with Cu content. The FeCoCr and Cu exhibit significantly different TC of about 13 and 397 $W \cdot m^{-1} \cdot K^{-1}$, respectively. Hence, the TC of CuFeCoCr composites strongly depends on Cu content, which is accomplished by the movement of electrons. In the composites with low Cu content (less than 45 wt%), it is hard to form a continuous net microstructure (shown in Fig.4a and 4b) as an unobstructed thermal conduction channel, resulting in a low TC. However, for the Cu50 and Cu60 composites, the interconnect matrix of the composites is changed as Cu-rich phase with the increase of Cu content, then improving their TC.

Fig.9 shows the measured Vickers hardness (HV) for Cu30-Cu65 composites. The error bars of HV are below 5% and the slight offset may be caused by experimental errors in the test process. Due to the increase of the low hardness Cu-rich phase, it is easy to understand that the HV value decreases linearly from 2640±100 MPa to 1600 ±150 MPa for the composites from Cu30 to Cu65, respectively. In addition, the HV of the composites decreases after annealing, which is attributed to

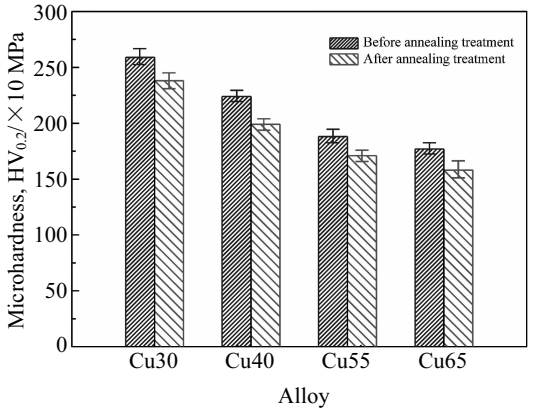

Fig.9 Microhardness of sintered $Cu_x(Fe_{0.37}Co_{0.54}Cr_{0.09})_{100-x}$ (x=30, 40, 55, 65, wt%) composite powders before and after annealing treatment

the decrease of the interfacial thermal stress after annealing.

3 Conclusions

1) A series of isotropic two-phase bulk composites consisting of Cu-rich and FeCoCr-rich phases are fabricated after sintering the composite powders at 900 °C.

2) The thermal expansion coefficients (CTE) of the CuFeCoCr composites increase with the increase of Cu content. And further annealing treatments based on the calculated phase diagram are expected to reduce the thermal expansion coefficients of CuFeCoCr and to improve thermal conductivities (TC).

3) The $Cu_{55}(Fe_{0.37}Cr_{0.09}Co_{0.54})_{45}$ composites exhibit excellent comprehensive properties with a CTE of 9.08×10^{-6} K^{-1} and a TC of 91.09 $W \cdot m^{-1} \cdot K^{-1}$ after annealing treatment, which match well with the properties of semiconductor for electronic packaging.

4) The simple synthesis and processing methods outlined here may prove to be effective methods for producing CuFeCoCr alloys used as low CTE-high TC materials in other applications.

References

1 Zweben C. *Journal of the Minerals, Metals & Materials Society*[J], 1998, 50(6): 47
2 Shen Y L, Needleman A, Suresh S. *Metallurgical & Materials Transactions A*[J], 1994, 25(4): 839
3 Zweben C. *Advanced Packaging Materials: Processes, Properties and Interfaces*[C]. Braselton: IEEE, 2001: 360
4 Yang H J Wang Z F, Wang H S *et al*. *Materials Review*[J], 2004, 18(6): 86 (in Chinese)
5 Ryelandt S, Mertens A, Delannay F. *Materials & Design*[J], 2015, 85: 318
6 Zhang Y J, Wang Z F, Lv W J *et al*. *Materials Review*[J], 1997, 11(3): 52 (in Chinese)
7 Yu X B, Wu R J, Zhang G D. *Materials Review*[J], 1994(3): 64 (in Chinese)
8 Li Q L, Hu D C. *Mechanical Management and Development*[J], 2007, 48(7): 1815 (in Chinese)
9 Tong Z S, Sheng Z S. *Electronics & Packaging*[J], 2005, 5(3): 6 (in Chinese)
10 Guo M, Liu J, Li Y. *Transactions of Nonferrous Metals Society of China*[J], 2014, 24(4): 1039
11 Zhu M, Shun L I, Xun Z *et al*. *Transactions of Nonferrous Metals Society of China*[J], 2014, 24(4): 1032
12 Wu G, Cheng Y, Wang K *et al*. *Journal of Materials Science: Materials in Electronics*[J], 2016, 27(6): 5592
13 Xu S, Habib A H, Pickel A D *et al*. *Progress in Materials Science*[J], 2015, 67: 95
14 Feng Y, Burkett S L. *Computational Materials Science*[J], 2015, 97: 1
15 Cai H, Wang Y P, Song X P *et al*. *Materials Review*[J], 2009, 23(15): 24 (in Chinese)
16 Cheng T Y, Xiong N, Cheng W U *et al*. *Materials for Mechanical Engineering*[J], 2010, 34(3): 38 (in Chinese)
17 Dan W U, Lei Y, Shi C *et al*. *Transactions of Nonferrous Metals Society of China*[J], 2015, 25(6): 1995
18 Wu D, Wu S P, Yang L *et al*. *Powder Metallurgy*[J], 2015, 58(2): 100
19 Wang C P, Liu X J, Jiang M *et al*. *Journal of Physics & Chemistry of Solids*[J], 2005, 66(2-4): 256
20 Liu X J, Wang C P, Gan S X *et al*. *Chinese Journal of Nonferrous Metals*[J], 2011, 21(10): 2511 (in Chinese)
21 Wang C P, Liu X J, Kainuma R *et al*. *Metallurgical & Materials Transactions A*[J], 2004, 35(4): 1243
22 Wang C P, Liu X J, Ohnuma I *et al*. *Science*[J], 2002, 297(5583): 990
23 Yu Y, Takaku Y, Nagasako M *et al*. *Intermetallics*[J], 2012, 25: 95
24 Wang C P, Liu X J, Ohnuma I *et al*. *Journal of Materials Research*[J], 2008, 23(4): 933
25 Takeuchi A, Inoue A. *Materials Transactions*[J], 2005, 46(12): 2817
26 Fahmy A A, Ragai A N. *Journal of Applied Physics*[J], 1970, 41(13): 5108

热压烧结制备 Cu/FeCoCr 复合材料的显微组织及热物理性能

刘兴军[1,2]，朱家华[1]，何洲峰[1]，张锦彬[1]，杨水源[1]，韩佳甲[1]，卢　勇[1]，王翠萍[1]

(1. 厦门大学 福建省材料基因工程重点实验室，福建 厦门 361005)

(2. 哈尔滨工业大学，广东 深圳 518055)

摘　要：利用相图计算的 CALPHAD 方法和超音雾化制粉技术，在 CuFeCoCr 体系中设计并制备了一系列微米级复合粉体。通过热压烧结方法在烧结温度为 950 ℃，烧结压力为 45 MPa 的工艺条件下成功获得块体复合材料。研究了块体复合材料中 Cu 含量对显微组织，热导率，热膨胀系数以及显微硬度的影响。结果表明：CuFeCoCr 块体复合材料均由 fcc 富铜相和 fcc 富铁钴铬相组成。该系列复合材料经 600 ℃时效处理 8 h 后，其热膨胀系数变化范围为 5.83×10^{-6}~10.61×10^{-6} K^{-1}，热导率变化范围为 42.17~107.53 $W\cdot m^{-1}\cdot K^{-1}$。其中 $Cu_{55}(Fe_{0.37}Cr_{0.09}Co_{0.54})_{45}$ 复合材料表现出良好的综合性能，即其热膨胀系数和热导率分别为 9.08×10^{-6} K^{-1} 和 91.09 $W\cdot m^{-1}\cdot K^{-1}$，与电子封装半导体材料的热膨胀系数相匹配。

关键词：CALPHAD 方法；复合材料；液相分离；热膨胀系数；热导率

作者简介：刘兴军，男，1962 年生，博士，教授，厦门大学材料学院，福建 厦门 361005，电话：0592-2187888，E-mail: lxj@xmu.edu.cn